FERMILAB-CONF-08-327-AD-APC-CD-E-TD

July 2008
SLAC-PUB-13319

Design and optimization of large accelerator systems through high-fidelity electromagnetic simulations

Cho Ng[1], Volkan Akcelik[1], Arno Candel[1], Sheng Chen[1], Lixin Ge[1], Andreas Kabel[1], Lie-Quan Lee[1], Zenghai Li[1], Ernesto Prudencio[1], Greg Schussman[1], Ravi Uplenchwar[1], Liling Xiao[1], Kwok Ko[1], T. Austin[2], J.R. Cary[2], S. Ovtchinnikov[2], D.N. Smith[2], G.R. Werner[2], and L. Bellantoni[3]

[1]Stanford Linear Accelerator Center, 2575 Sand Hill Road, Menlo Park, CA 94025
[2]TechX Corporation, 5621 Arapahoe Ave, Suite A, Boulder, CO 80303
[3]Fermilab, P.O. Box 500, Batavia, IL 60510-5011

SciDAC CETs/Institutes Collaborators: E. Ng, X. Li, C. Yang (LBNL), L. Dianchin (LLNL), K. Devine, E. Boman (SNL), B. Osting, D. Keyes (Columbia), X. Luo, M. Shephard (RPI), R. Barrett, S. Hodson, R. Kendall (ORNL), W. Gropp (ANL), Z. Bai, K.-L. Ma (UC Davis)

Email: cho@slac.stanford.edu

Abstract. SciDAC1, with its support for the "Advanced Computing for 21st Century Accelerator Science and Technology" (AST) project, witnessed dramatic advances in electromagnetic (EM) simulations for the design and optimization of important accelerators across the Office of Science. In SciDAC2, EM simulations continue to play an important role in the "Community Petascale Project for Accelerator Science and Simulation" (ComPASS), through close collaborations with SciDAC CETs/Institutes in computational science. Existing codes will be improved and new multi-physics tools will be developed to model large accelerator systems with unprecedented realism and high accuracy using computing resources at petascale. These tools aim at targeting the most challenging problems facing the ComPASS project. Supported by advances in computational science research, they have been successfully applied to the International Linear Collider (ILC) and the Large Hadron Collider (LHC) in High Energy Physics (HEP), the JLab 12-GeV Upgrade in Nuclear Physics (NP), as well as the Spallation Neutron Source (SNS) and the Linac Coherent Light Source (LCLS) in Basic Energy Sciences (BES).

1. Introduction

Particle accelerators are important experimental facilities in DOE for discoveries in physical sciences. In the high energy frontier, particle colliders such as the proposed International Linear Collider (ILC) will be used to address many of the most compelling questions about dark matter, dark energy, and the fundamental nature of matter, energy, space and time. In basic energy sciences research, high-intensity particle beams or high-brightness light sources generated by particle accelerators will probe structures of matter that will benefit science discoveries in biology, chemistry, medical sciences, material sciences and others. Examples of these machines are the Spallation Neutron Source (SNS) and the

Work supported in part by US Department of Energy contract DE-AC02-76SF00515
Invited talk presented at the SciDAC 2008, 7/13/2008 to 7/17/2008, Seattle, WA, USA

Linac Coherent Light Source (LCLS). Central to these billion-dollar class, state-of-the-art accelerators are accelerator structures used to accelerate particle beams to high energies. Under the support of SciDAC, advanced electromagnetic simulation tools have been developed for the design and optimization of accelerator structures [1], with the objectives of achieving improved performance, increased reliability and reduced cost of accelerators.

In SciDAC1, EM modeling [2] in the AST project made dramatic advances in the development of parallel, high-fidelity, and high-accuracy finite-element codes at the Stanford Linear Accelerator Center (SLAC). The application of these codes has tremendous impact on the design, optimization and analysis of accelerator projects within the Office of Science. For example, AST EM modeling tools were used to simulate beam heating in the PEP-II (an HEP accelerator) interaction region (IR) and the analysis led to a redesign of the IR, resulting in higher luminosity which enabled the discovery of a new elementary particle. The successes of large-scale EM modeling would not have been possible without the computational expertise rendered by ISICs/SAPP partners, especially in the areas of unstructured mesh generation, adaptive mesh refinements, eigensolvers, parallel partition schemes and visualization [3]. For instance, the finite-element eigensolver Omega3P saw a thousand times speedup through collaborations with ICIS Center TOPS on novel parallel algorithms in eigensolvers and linear solvers.

Following the successes of EM modeling in AST, the ComPASS [4] EM team will continue to strive for advances in accelerator simulation techniques and capabilities that will take advantage of petascale computer hardware in SciDAC2. The finite-element tools using unstructured grids developed in SciDAC1 will be augmented to include self-consistent particle-wave interactions and multi-physics analysis that integrates EM, thermal and mechanical effects for accelerator cavity design. In particular, the multi-physics analysis aims at engineering prototyping of accelerator components on computers with unprecedented realism and resolution through petascale modeling, resulting in a fast turnaround time that will revolutionize the current design cycle. The ComPASS EM efforts will also be augmented by the finite-difference time-domain (FDTD) method using a structured mesh approach, which allows for conformal, embedded boundaries for modeling curved surfaces. Collaborations with SciDAC CETs/Institutes in computational science will continue in existing areas and new areas (such as shape determination) to develop scalable numerical algorithms and advanced numerical analysis techniques to facilitate large-scale simulations on petascale computers. It is envisioned that ComPASS EM tools will tackle the most computationally challenging problems in accelerators across the Office of Science, as can be gleaned from the very first applications of ComPASS described in following sections.

2. Parallel Electromagnetic Codes for High-Fidelity Simulations

The parallel EM codes [2, 3] developed in the AST project at SLAC were based on the finite-element method using unstructured grids to conform to complicated geometry and high-order basis functions to achieve high solution accuracy, more than that obtained by precise machining of cavities. The suite of finite-element codes include

- Omega3P – Parallel eigensolver for finding normal modes and their damping in accelerating cavities
- S3P – Parallel S-matrix calculation for computing transmission properties of accelerator structures
- T3P – Parallel time-domain solver with beam excitation for wakefield calculations
- Track3P – Parallel particle tracking module for multipacting and dark current simulations
- V3D – Graphic tool for visualizing meshes, fields and particles with unstructured grids

In addition to improving the computational capabilities of these codes, two new codes for treatments of different space-charge effects and a novel multi-physics code with its relevant solvers all based on the finite-element method will be developed in ComPASS. They are

- Gun3P – Parallel particle code for space charge beam optics for electron gun simulations
- Pic3P – Parallel particle-in-cell code for radio-frequency (rf) gun and klystron simulations

- TEM3P – Parallel multi-physics analysis tool including integrated EM, thermal and mechanical effects for cavity design

For the FDTD approach, VORPAL, developed by TechX, uses the Dey-Mittra algorithm [5] for accurate incorporation of boundaries. This is an *embedded boundary* algorithm, which uses a structured mesh throughout most of the simulated region but modifies the cells near the boundary only to obtain improved accuracy. To extract frequencies, we developed an efficient method [6] that combines targeted excitation with filter diagonalization. This allows one to reduce the eigenvalue problem to a small subspace, thus eliminating the need to diagonalize large matrices. Combined with massive parallelism, this provides the ability to cover the scales of cavities from the full size of a multicell cavity down to the tiny holes through which diagnostics are inserted.

3. Collaborations in Computational Science with SciDAC CETs/Institutes

Strong collaborations have been established between ComPASS and SciDAC CETs/Institutes. The collaborations include the following R&D activities.

- *Shape Determination & Optimization* (with ITAPS and TOPS) – Obtain cavity deformation from measured mode data by solving a weighted least squares minimization problem
- *Parallel Complex Nonlinear Eigensolver and Linear Solver* (with TOPS) – Develop scalable algorithms for solving large, complex, nonlinear eigenvalue problems to find mode damping for accelerator systems, and for solving highly indefinite systems arising from accelerator modeling
- *Adaptive Mesh Refinement and Meshing Service* [7] (with ITAPS) – Optimize computing resources and increase solution accuracy through adaptive mesh refinement
- *Dynamic Load Balancing* (with CSCAPES [8] and ITAPS) – Implement dynamic partitioning scheme to optimize computational load for particle-field simulations
- *Parallel and Interactive Visualization* (with ISUV) – Visualize electromagnetic fields and particles with large, complex geometries and large aspect ratios
- *Embedded Boundary Methods* (with ITAPS) – Extend the integration of embedded boundary methods with particle-in-cell codes using structured grids

All but the last collaboration are applicable to the finite-element method using unstructured grids. Details on these efforts are described in these proceedings in a separate paper [9]. The importance of the collaborative work will also be illustrated in the following EM applications.

4. Application to Accelerator Projects in High Energy Physics

(1) Simulation of the ILC Cryomodule [10]

The determination of wakefield and higher-order-mode (HOM) effects is of utmost importance in the design of the ILC linacs. Previous calculations had been carried out for a single superconducting cavity where the spectrum and the damping factors of HOMs were obtained using the parallel finite-element eigensolver Omega3P [1]. The calculations assumed that the frequencies of the HOMs are below the cutoff frequency of the beampipe. For HOMs above the cutoff, the fields may cover regions more than a single cavity, and therefore calculations involving multiple cavities are required to give a correct account of wakefield effects of these modes. To determine trapped modes and their effects on the wakefield, we modeled the ILC cryomodule, which consists of eight TTF cavities.

In the frequency domain, we used Omega3P to calculate the trapped modes in the cryomodule for the third dipole band, for mode frequencies above the beampipe cutoff frequency. Sixteen dipole modes with high shunt impedances were evaluated and the calculated damping factors agreed reasonably well with the data measured for cryomodules at DESY. This was the first-ever calculation of trapped modes in the cryomodule. An example dipole mode is shown in Fig. 1. Each mode took about one hour with 1500 processors on the Seaborg computer at NERSC. The calculations were facilitated by advances in parallel linear solvers (with TOPS) so the linear systems resulting from the large computational size of the cryomodule could be solved efficiently on the NERSC machine. A new

multi-mode waveguide boundary condition was also implemented in Omega3P to properly terminate the modes at the two ends of the cryomodule. The Maxwell system becomes a nonlinear complex eigenvalue problem, which may be solved using a self-consistent iterative algorithm.

Figure 1. A mode in the third dipole band in the ILC cryomodule obtained from Omega3P. Note that the field pattern rotates along the cryomodule because of the 3-dimensional effects of the couplers located in the interconnecting beampipes. This may produce unwanted x-y wakefield couplings.

In the time domain, we used the finite-element code T3P to drive a Gaussian bunch through the cryomodule. A snapshot of the beam transit in the cryomodule using the visualization tool V3D is shown in Fig. 2. The Fourier transform of a monitored signal at the beampipe between two cavities shows a sharp peak close to the monopole cutoff frequency of the beampipe. To further determine the nature of this peak, we used Omega3P to solve for modes at frequencies around the peak, and a localized mode was found in the coupler region between two cavities (see Fig. 3). The shunt impedance and damping factor of this mode indicate that the heat load it generates on the beampipe wall is relatively small and should not be a concern for the ILC linacs.

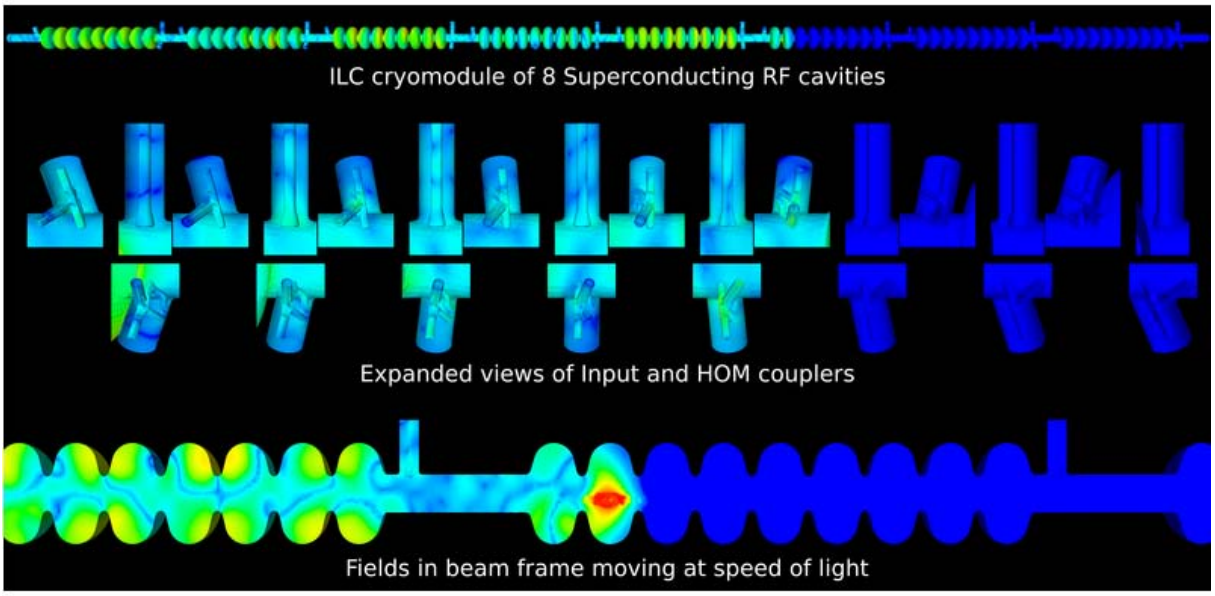

Figure 2. A T3P snapshot of wakefield generated by an electron bunch traversing ILC cryomodule.

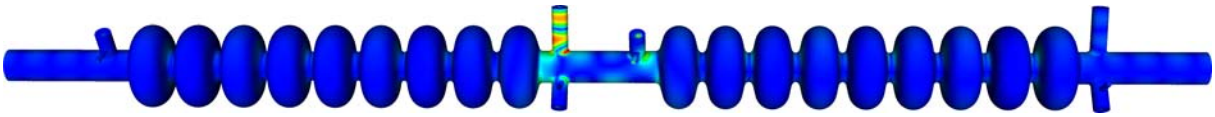

Figure 3. A trapped mode in the region between two cavities of the ILC cryomodule using Omega3P.

(2) Multipacting in ILC TTF-III coupler [11]

The TTF-III power coupler adopted for the ILC baseline cavity design tends to have a long initial high power processing time. The long processing time is believed to result from multipacting in various regions of the coupler. Multipacting is a phenomenon arising from electrons with resonant trajectories hitting a cavity surface at same locations leading to an avalanche of electron currents that will hinder the cavity performance. To understand performance limitations during high power processing and identify problematic regions, SLAC built a flexible high-power coupler test stand to test individual sections of the coupler, including the cold and warm coaxes, the cold and warm bellows, and the cold window. To provide insights for the high power test, detailed numerical simulations of multipacting

for these sections were performed using Track3P. Multipacting bands were identified by scanning power levels up to 2 MW. For the cold coax, the simulated multipacting bands agreed very well with measurements (see Fig. 4). Multipacting activities were found in the taper region, but they could be suppressed by applying an axial magnetic field above 300 Gauss. Multipacting activity was not apparent at the bellows.

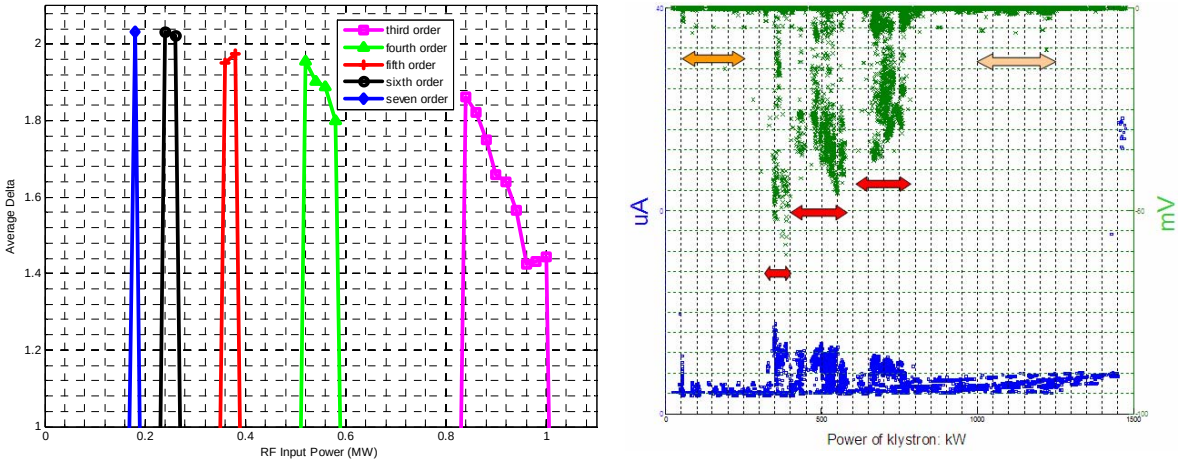

Figure 4. Multipacting activities in the cold coax of the TTF coupler: (Left) Multipacting bands obtained from Track3P; (Right) Electric current measured at a probe during high-power processing.

(3) Impedance calculations for the ILC damping rings [12]

The goals of the impedance calculation for the ILC damping rings are to obtain the impedance budget for the vacuum chamber components and to provide a pseudo-Green's function wakefield for beam stability studies. The evaluation of the pseudo-Green's function wakefield necessitates the accurate determination of the short-range wakefield using a bunch length much smaller than the normal bunch length. As the bunch length gets smaller, the computational size becomes larger because the mesh requires refinement to handle the high frequency content of the short bunch.

The conceptual designs of the ILC damping vacuum chamber components were obtained by scaling those in existing machines such as the PEP-II. We used the parallel time-domain code T3P to calculate the pseudo-Green functions of the major vacuum chamber components such as the rf cavity and the beam position monitor (BPM) using a 1 mm bunch (compared with the nominal bunch length of 6 mm). The calculations were carried out on the Bassi computer at NERSC. Fig. 5 shows the field pattern and the pseudo-Green's function wakefield due to the beam transit through the BPM.

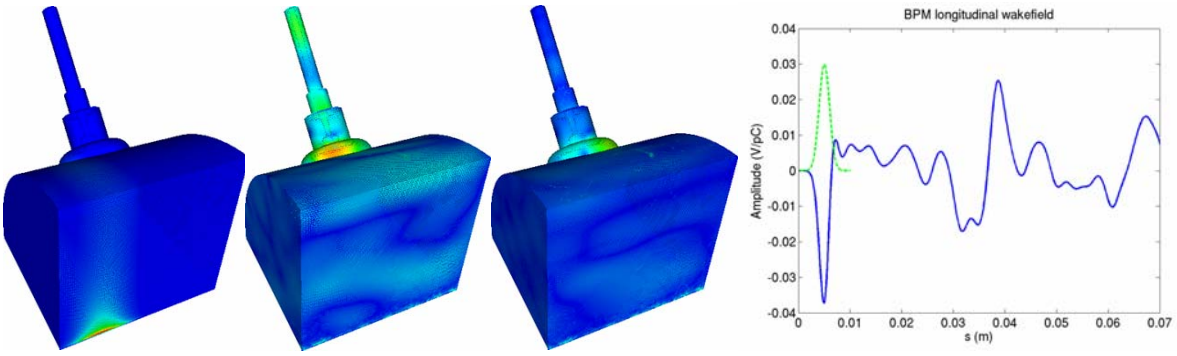

Figure 5. (Left) Transit of a Gaussian bunch through the BPM using T3P; (Right) Pseudo-Green's function wakefield for a 1 mm RMS bunch.

It is desirable to obtain the pseudo-Green's function wakefield for even smaller bunch lengths for more accurate beam stability studies. However, the computational requirements would become

prohibitively high. The difficulty can be alleviated by introducing a computational window moving along with the bunch because the short-range wakefield receives contributions only from fields in the longitudinal region covered by the bunch. The two proposed approaches are to have a moving window with p-refinement and a moving window with h-refinement. In the p-refinement method, high-order finite elements are used in the moving window to improve the solution accuracy, and the region outside the window is represented by lowest order finite elements. This drastically reduces the problem size and preliminary studies have shown that CPU time can be reduced by an order of magnitude, compared to using basis functions of uniform order. In the h-refinement method, the moving window has a much more refined grid than the region outside the window. Collaboration with RPI (ITAPS) is in progress for moving window with h-refinement to obtain high-quality meshes for computation.

(4) ILC Crab Cavity

One of the tasks of the last year has been to carry out verification and validation studies. The first such (verification) study was to re-compute the frequency spectrum of the "crab cavity" to be used for the final beam delivery system to enhance the luminosity at the interaction point of the proposed International Linear Collider (ILC). Our results differed from previous (obtained with the MAFIA code) by 3 MHz out of 3.9 GHz. This 0.1% error in most fields of physics would not be significant, but cavity frequencies can be measured to parts in 10^5, so it was worth understanding.

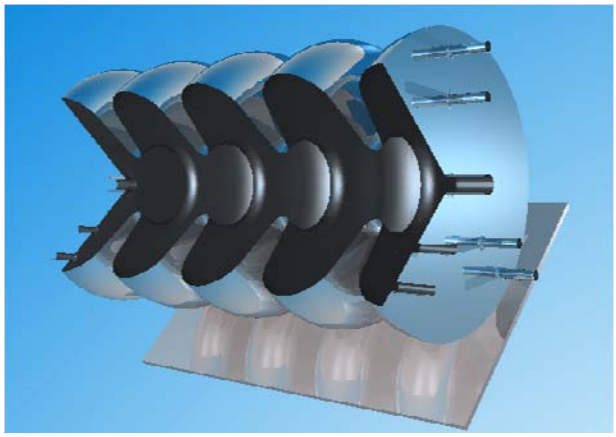

Figure 6. Visualization of the A15 cavity experiment as represented within VORPAL.

Experiments could not act as arbiter in this case, because the superconducting cavities in question cannot be manufactured to sufficiently high accuracy. So instead we developed computations for the precisely machined A15 cavity experiment shown in Fig. 6. This had long been a curiosity, because previous calculations had differed from experimental results by 5 MHz. After extensive checking, including modeling all of the holes in the cavity, our results also disagreed, but by 2 MHz, which was still unacceptable. Ultimately, we carried out computations for differing values of cavity dimensions and determined that a reduction of the equator radius by 25 μm could account for the observed frequency shift. This led to an as-is measurement of the manufactured cavities, and, indeed, the radius of the equator was found to be smaller by 25 μm, as indicated by the computations. Thus we can say that at this point our cavity calculations have been both verified and validated to within a part in 10^4.

5. Application to Accelerator Projects in Nuclear Physics

High-Q resonances in JLab high gradient prototype cryomodule [13]

The *Renascence* cryomodule installed in CEBAF in 2007 consists of 8 superconducting cavities. Beam-based instability studies have shown a significant beam breakup (BBU) threshold current well below the designed value. Measurements of higher-order modes (HOM) indicate that three of the modes in cavity #5 have external Qs two orders of magnitude higher than similar modes in other cavities. It is important to understand the cause of this abnormal behavior so that effective QC measures can be implemented to avoid the BBU problem in the final upgrade design and manufacture.

The abnormality exhibited by cavity #5 could arise from shape deviations of the real cavity from the designed one. However, deviations are unknown in the final cavity installation because of the complicated process of assembly and tuning. The ability to reconstruct the deformed cavity from

measured data will provide valuable information for cavity design and performance. Thanks to the support of the Office of Advanced Scientific Computing Research (ASCR) and the collaboration with TOPS scientists, SLAC physicists and computational scientists have developed a shape determination tool to determine the unknown shape deviations using measured cavity rf parameters such as mode frequencies and external Qs by solving an inverse problem [14]. The algorithm is based on the least squares minimization, whose goal is to find the best shape that minimizes the least squares misfit between the measured and simulated models. The shape deviations in the simulated model are parameterized using predefined geometry parameters, and the inversion of the problem quantifies these parameters to determine the reconstructed, deformed shape.

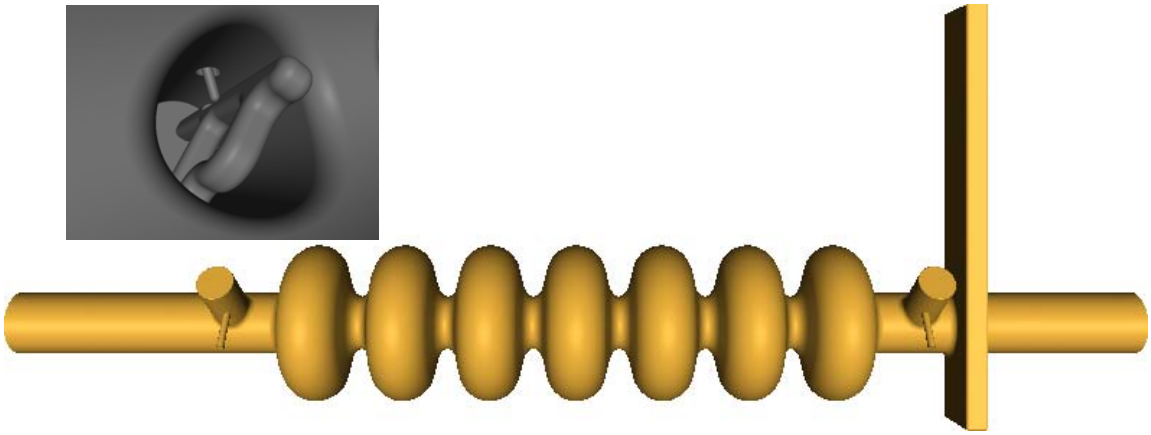

Figure 7. The 7-cell high gradient cavity model with details of HOM coupler (insert).

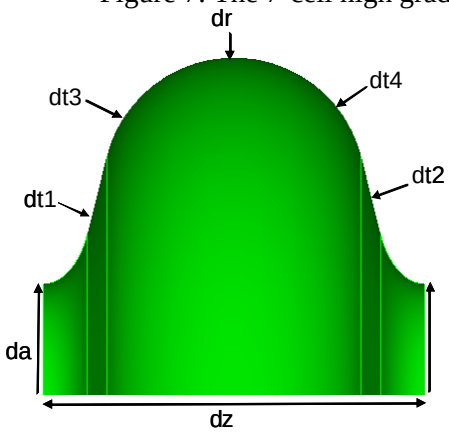

Figure 8. Distortion parameters used in shape determination.

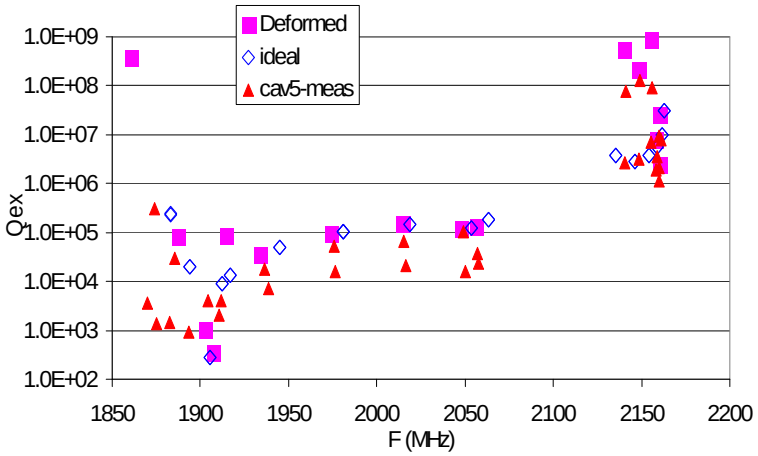

Figure 9. Q_{ext} for ideal and deformed cavities using Omega3P.

The first step of the shape determination is to parameterize each cavity cell with predefined distortion parameters as shown in Fig. 8. The subsequent goal is to determine the deformed cavity shape by variations of these distortion parameters to achieve the optimal fit to measured cavity rf parameters, which include the 7 monopole mode frequencies, 12 dipole mode frequencies and 6 external Q (Q_{ext}) values. Fig. 9 shows the Q_{ext}'s of dipole modes of the deformed cavity after applying the shape determination tool. Also plotted are the measured data for cavity #5, and those for the ideal designed cavity using Omega3P. The deformed shape not only reproduces the 3 high Q_{ext} modes ($Q_{ext} \sim 10^8$ and frequency ~ 2160 MHz) in the second dipole band, but also the low Q_{ext} modes for the remaining modes in the second dipole band and for the modes in the first band (~ 1850-2050 MHz). The dominant cavity distortion is found to be the distortion in the cell length (dz), and some cells are shorter by 2-3 mm. The total length of the deformed 7-cell cavity is 8.2 mm shorter than that of the ideal design, which is in good agreement with the QC data of cavity #5.

Inspections of the field patterns of these 3 high-Q modes of the deformed cavity show that their field patterns are substantially different from the corresponding modes of the ideal cavity. The reduced couplings of these high-Q modes in the deformed cavity decrease their damping effects, which then leads to the BBU problem. The cell shapes of the deformed cavity from the ideal one is illustrated in Fig. 10.

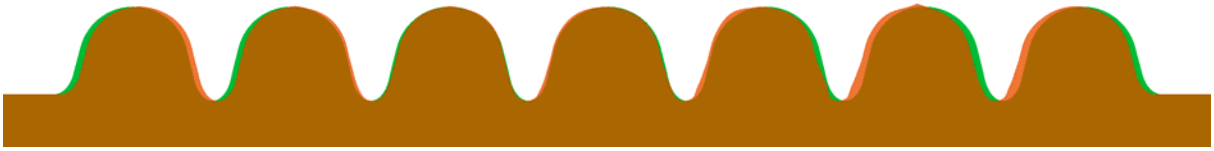

Figure 10. Overlay of distorted cavity (in pink color) on ideal cavity (in green color) (common region in orange color).

6. Application to Accelerator Projects in Basic Energy Sciences

Multipacting simulation for HOM coupler in SNS superconducting cavity [15]

During the commissioning and operation of the SNS superconducting linac, abnormal signals were observed at the HOM coupler. These anomalies are believed to be due to the field emission and multipacting electron loadings in the HOM coupler. To understand these issues, the field enhancement and multipacting were simulated using Omega3P and Track3P for the SNS beta=0.81 cavity. The high field gradient in the upstream HOM coupler could cause field emission and multipacting (MP). Multipacting analysis using Track3P shows two multipacting bands in the gradient range up to 20 MV/m. One of the multipacting bands exists in the gap between the enlarged loop head and the cylindrical side wall of the coupler at field gradient levels from 2.8 to 10 MV/m as shown on the left of Fig. 11. The other MP band exists in the gap between the hook part of the loop and the cylindrical side wall of the coupler as shown on the right of Fig. 11. No MP activities are found in the notch gap. These MP bands are in good agreement with the experimental observations.

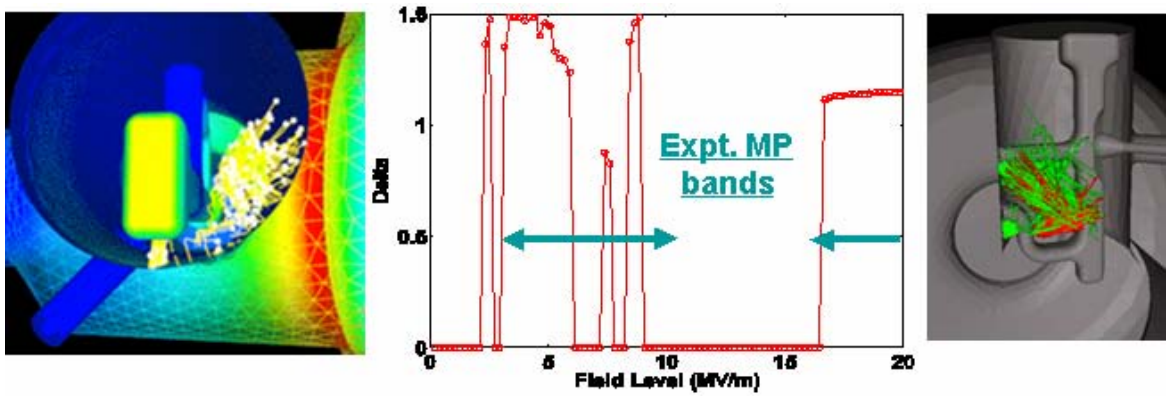

Figure 11. Multipacting activities in the SNS HOM coupler from Track3P simulation.

7. Multi-physics Analysis for Engineering Prototyping

In the design of an accelerator cavity, thermal and mechanical considerations are as important as EM effects. Many failures in accelerator operations are due to heating effects arising from high power or high current operations. Presently, the EM, thermal and mechanical calculations are carried out separately with different codes using different meshes. It is highly desirable in the accelerator community to build a modeling package that integrates all these effects. Under ComPASS, a new thermal and a new mechanical solver will be developed and integrated into existing EM codes. Traditionally, thermal and mechanical analysis tools use the finite-element method, and hence it is natural to integrate them into the ComPASS finite-element EM suite. The multi-physics analysis code TEM3P will enable all these calculations to be done within a unified framework using a single model and will provide a complete toolset for engineering prototyping.

To illustrate how TEM3P is used for engineering prototyping, we use the LCLS rf gun as an example [16]. The analysis starts with a CAD model of the rf gun as shown in Fig. 12. The CAD model contains 2 regions: the vacuum region (pink) used for EM computation, and the cavity metallic walls with detailed cooling channel layout (yellow) for thermal and mechanical analysis. In an integrated analysis process, the EM eigensolver Omega3P is used to calculate the accelerating mode of the cavity (Fig. 13a). The rf power loss on the cavity walls is then used as input to the thermal solver to find the temperature distribution inside the cavity wall thickness (Fig. 13b). The temperature distribution on the cavity wall boundaries is then input to the mechanical solver to calculate the wall distortion and stress distribution (Fig. 13c). The subsequent distorted cavity due to thermal and mechanical effects is used by the EM eigensolver Omega3P again to determine the frequency shift of the accelerating mode. The analysis process is repeated until an acceptable design is obtained.

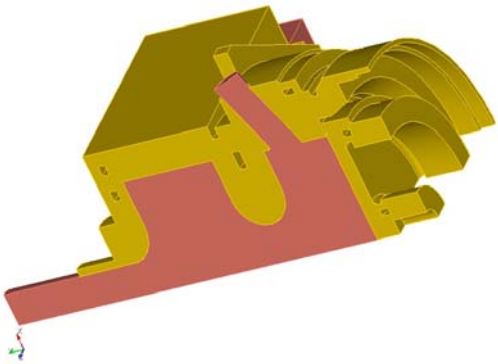

Figure 12. CAD model of LCLS rf gun.

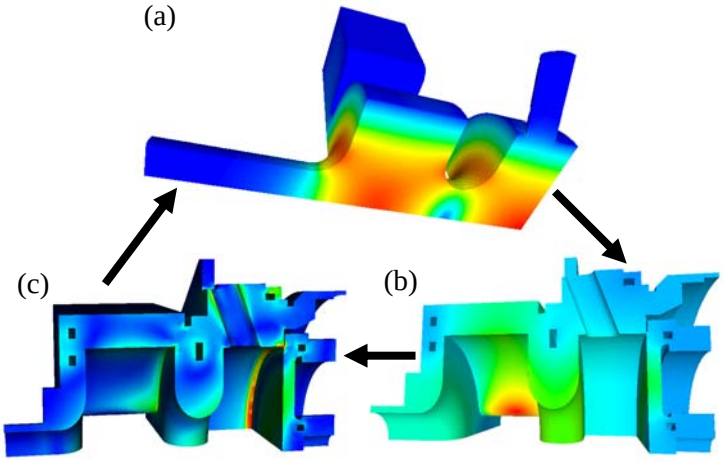

Figure 13. (a) EM field ; (b) temperature; (c) mechanical stress distributions from TEM3P.

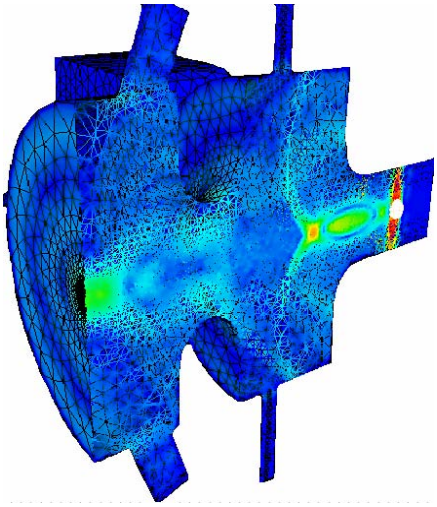

Figure 14. Beam transit in LCLS rf gun using Pic3P

The complete design of the rf gun also needs to satisfy beam dynamic requirements. The beam emittance of the rf gun can be evaluated with the same mesh using Pic3P in the ComPASS finite-element suite. Pic3P, first of its kind, is a 3D parellel finite-element particle-in-cell code which includes wakefield and retardation effects that are generally ignored in standard space-charge tracking codes. It has been optimized specifically for highly efficient rf gun simulations employing various novel computational techniques [17]. Fig. 14 shows a snapshot of the scattered fields excited by the transit of a bunch using Pic3P. Fig. 15 shows the beam emittance obtained using Pic3P.

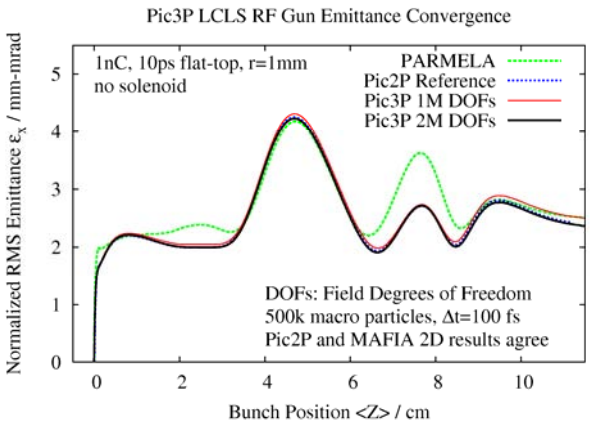

Figure 15. Beam emittance of LCLS rf gun using Pic3P.

8. Summary

Electromagnetic modeling has seen tremendous advances in SciDAC1 AST project, and will continue to play an important role in ComPASS in tackling the most computational challenging accelerator problems in HEP, NP and BES across the Office of Science. With ASCR and SciDAC CETs/Institutes support, the computational tools, developed through concerted efforts from applied mathematicians, computer scientists and accelerator physicists, have demonstrated their impacts on the design and optimization of accelerators to ensure their performance and reliability while maintaining low costs.

Acknowledgments

We are grateful to H. Wang, F. Marhauser, J. Sekutowicz, C. Reece and R. Rimmer of TJNAF for initiating the BBU problem in a CEBAF cryomodule and for supplying all the relevant measured data. This work was supported by the U.S. Department of Energy Office of High Energy Physics, Office of Basic Energy Sciences and Office of Advanced Scientific Computing Research under contract DE-AC02-76SF00515 and grants DE-FC02-07ER41499 and DE-FG02-04ER41317. This work used resources of the National Center for Computational Sciences at Oak Ridge National Laboratory and resources of the National Energy Research Scientific Computing Center, which are supported by the Office of Science of the Department of Energy under Contract DE-AC05-00OR22725 and DE-AC02-05CH11231, respectively.

References

[1] C. Ng et al., "State of the Art in EM Field Computation", Proc. of EPAC2006, Edinburgh, UK, June 26-30, 2006.

[2] K. Ko et al., "Impact of SciDAC on Accelerator Projects across the Office of Science through Electromagnetic Modeling", J. of Physics, **16**, 195 (2005).

[3] L.-Q. Lee et al., "Advancing Computational Science Research for Accelerator Design and Optimization", Proc. of SciDAC 2006 Conference, Denver, Colorado, June 25-29, 2006.

[4] P. Spentzouris et al., "Community Petascale Project for Accelerator Simulation: Advancing Computational Science for Future Accelerators and Accelerator Technologies", these proceedings.

[5] S. Dey and R. Mittra, IEEE Microwave and Guided Wave Lett., 7, 273 (1997).

[6] G.R. Werner and J.R. Cary, J. Comput. Phys., **227**, 5200 (2008).

[7] M. Shephard, "Curved Mesh Correction and Adaptation Tool to Improve ComPASS Electromagnetic Analysis", these proceedings.

[8] A. Pothen, "The CSCAPES Institute: Recent Progress", these proceedings.

[9] L.-Q. Lee et al., "Computational Science Research in Support of Petascale Electromagnetic Modeling", these proceedings.

[10] L.-Q. Lee et al., "Multi-Cavity Trapped Mode Simulation", talk given at Wake Fest 07 Workshop, Stanford, December 18-20, 2007.

[11] L. Ge et al., "Multipacting Simulations of TTF-III Coupler Components", Proc. of PAC2007, Albuquerque, New Mexico, June 25-29, 2007.

[12] C. Ng, "Status and Plans for the Impedance Calculations of the ILC Damping Rings", talk given at ILC Damping Rings Mini-Workshop, KEK, Tsukuba, Japan, December 18-20, 2007.

[13] R. Kazimi et al., "Observation and Mitigation of Multipass BBU in CEBAF", Proc. of EPAC2008, to appear.

[14] V. Akcelik et al., "Maxwell Eigenvalue Determination for Deformed Cavities", J. Comput. Phys., **227**, 1722 (2008).

[15] Z. Li et al., "Towards Simulations of Electromagnetics and Beam Physics at the Petascale", Proc. PAC2007, Albuquerque, New Mexico, June 25-29, 2007.

[16] V. Akcelik et al., "Parallel Computation of Integrated Electromagnetic, Thermal and Structural Effects for Accelerator Cavities", Proc. of EPAC2008, to appear.

[17] A. Candel, "Load Balancing of Parallel 3D Finite Element Particle-in-Cell Code Pic3P", talk given at CSCAPES Workshop, Santa Fe, New Mexico, June 10-13, 2008.